論文2001-38SP-3-2

도트 패턴 선택을 이용한 모델 기반 디더링

(Model-based Dithering Using Dot Pattern Selection)

李 採 守 *, 朴 洋 佑 *, 嚴 泰 億 **, 張 周 錫 **, 河 永 浩 **

(Chae-Soo Lee, Yang-Woo Park, Tae-Uk Uam, Joo-Seok Jang, and Yeong-Ho Ha)

요 약

일반적 칼라 출력 장치는 제한된 범위의 색만을 재현 할 수 있다. 특히 프린터와 같이 색의 재현성이 부족한 장비에서는 하드웨어 특성에 따른 채색 면적이나 인쇄에 사용되는 용지의 특성에 따라 염료의 확산 등에 대해서도 고려해야 한다. 특히, 색을 프린트하기 위해서는 출력 과정에서 색의 선형적인 증가와 감소가 이루어져야 하며 또한 정확한 색의 모델링이 가능하여야 한다. 따라서 본 논문에서는 이를 위해 프린터 출력 시 실제 채색 면적과 시각적 색감을 고려할 수 있는 디더링 방법을 제안한다. 제안된 방법은 실제 채색 면적을 고려한 패턴 데이터 베이스를 만들어 이를 디더링 패턴으로 이용하게 된다. 그리고 이 데이터 베이스에서 정확한 패턴을 선택하기 위해서는 인간시각의 색 인지력을 모델링한 대조 민감도 함수를 사용하게 된다. 따라서 본 논문에서는 저해상도의 칼라 출력장치에서도 고화질의 색을 재현할 수 있게 해준다.

Abstract

New methods are proposed for printing a full resolution image on a limited output device. The proposed algorithm uses a dot-pattern database that models overlapping phenomena among neighbor printing dots. To solve the problem of dot-overlap, the gray levels of dot-pattern sets were calculated using a circular dot-overlap model and then measured by a spectrometer. Thereafter, in order to improve the visual quality of the color dithering, the contrast sensitivity function of the human visual system was used. As a result, the optimal dot-pattern can be selected from the database. Consequently, the proposed algorithm can produce high quality images while using low-cost color devices.

* 正會員, 경운대학교 멀티미디어정보학부

(School of Multimedia, Visual Arts, and Software Engineering, Kyungwoon University)

** 正會員, 구미기능대학교 전자과

(Dept. of Electronic Technology, Kumi Polytechnic College)

*** 正會員, 경북대학교 전자전기공학부

(School of Electronic & Electrical Eng., Kyungpook National University)

※ Acknowledgement. "This work was supported by Korea Research Foundation Grant. (KRF-99-003-E00360)"

接受日字:2000年7月15日, 수정완료일:2001年12月22日

I. INTRODUCTION

Digital dithering is the process of generating a pattern of dots, within a limited number of levels, for the reproduction of a continuous tone image. Digital dithering is necessary for displaying continuous tone images in media when the direct rendition of tones is impossible. Accordingly, many dithering techniques are included in printing algorithms.[1~5] Conventional order dithering[1,6,7,9,10] uses linear quantization through which input gray levels are equally divided by the printer resolution. Each pixel is then thresholded

according to the value of its corresponding position in the dither matrix. This algorithm requires only simple processing and uses less computational time, however, it does not consider the hardware characteristics of the printer, therefore, differences in intensity are produced between a monitor and a printed image. In error diffusion[1,3,8], errors produced during quantization are diffused into the neighborhood to compensate the local gray level. These errors may then cause a decrease in contrast in an edge region and a color change in a neighboring region.

To solve these problems, model-based dithering of dot-pattern selection is proposed. The proposed algorithm uses a dot-pattern database that models overlapping phenomena among neighbor printing dots. A dot-pattern is defined as a part divided from a dot-profile which is the binary pattern resulting from the dithering of a constant gray level. In this paper, a dot-profile is generated using conventional blue noise masking. Therefore, the visual appearance of a dot pattern is similar to that of a dot-profile produced using blue noise masking. There are two steps involved in the proposed algorithm: the generation of a dot-pattern database and the selection of a dot-pattern from the dot-pattern database to represent the gray level. To solve the gray level difference problem, the gray levels of the dot-pattern sets are calculated using the circular dot-overlap model. Thereafter, the dot-pattern sets are reordered according to the results. In this paper, in order to improve the visual quality of the color dithering, the contrast sensitivity function (CSF) of the human visual system is used wherein the contrast sensitivity decreases rapidly with an increasing spatial frequency. Using this CSF, the visual difference between the original image and the dithered image can be computed as a numerical value. As a result, the optimal dot-pattern can be selected from the database. High quality printed images are produced with the proposed color dithering method and display less color degradation than conventional printing methods.

II. CONVENTIONAL DITHERING ALGORITHMS

1. Ordered-dither

Ordered-dither[1,6] is the natural digital solution, where a two-dimensional threshold array is designed and the halftoning process is accomplished by a simple pixelwise comparison of the gray scale image against the array (Fig. 1). This method is straightforward and requires little computational thus ordered-dither is the most popular and widely used technique. Depending on the progressive ordering of how halftone dots in a cell are turned on/off, ordered-dither can be classified into clustered-dot and dispersed-dot. In clustered-dot ordered-dither, adjacent pixels are turned on as gray level changes to form a cluster in the halftone cell. Clustered-dot dither is primarily used for printing devices that have difficulty printing isolated single pixels. Obviously, this congregation of pixels will result in noticeable low-frequency structures in the output image. On the other hand, in dispersed-dot

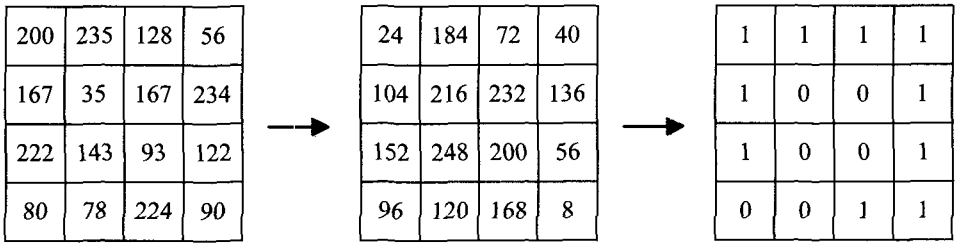

(a) Input gray image (b) Dither screen (c) Output binary image

Fig. 1. Ordered-dither halftoning technique.

ordered-dither, halftone dots in a cell are turned on individually without grouping them into clusters. Therefore, sharp edges can be better rendered compared to clustered-dot dither. However dispersed-dot techniques are more susceptible to dot gain.

2. Stochastic processes

Many problems of ordered-dither, including susceptibility to Moire patterns and highly visible texture, can be traced back to its rigid regular structures. To break these regular structures, researchers sought less obtrusive halftone patterns. Blue noise halftoning, also called stochastic screening or frequency modulated (FM) screening, has been the most active research field in digital halftoning in recent years. These terms have been loosely applied to both algorithm approaches and the screen approach. Error diffusion is the algorithm approach that has been most extensively studied, whereas the blue noise mask (BNM) is the term first applied to a screen or threshold array that produces unstructured, visually appealing halftone patterns. In order to follow a precise definition from now on, the term stochastic screening applies to a threshold array. Also, mask and screen will be used interchangeably when both will refer to a threshold array.

3. Error diffusion

Error diffusion is a popular method for generating sharp halftone images for output devices that do not display the substantial intensity. Floyd and Steinberg introduced this algorithm in 1976 as a method for computer displays. The method uses the concepts of calculating the error between input and binary output and incorporating this error in the calculation of subsequent output pixels. The component of the halftoned image is obtained by the following set of equations

$$\begin{aligned} v_{i,j} &= x_{i,j} - \sum_{m,n} h_{m,n} e_{i-m,j-n} \\ b_{i,j} &= \begin{cases} 0, & \text{if } v_{i,j} > t \\ 1, & \text{otherwise} \end{cases} \\ e_{i,j} &= (1 - b_{i,j}) - v_{i,j} \end{aligned} \quad (1)$$

where $v_{i,j}$ is the corrected value of the component of the continuous tone image. The error $e_{i,j}$ at any instant is defined as the difference between the corrected continuous tone image component and the halftone image component. The past errors are filtered and subtracted from the current image value $x_{i,j}$ before it is thresholded to obtain $b_{i,j}$. $h_{i,j}$ is the impulse response of the error-filter. The structure of the algorithm is shown in Fig. 2 and the error-filter used in this processing is shown Fig. 3.

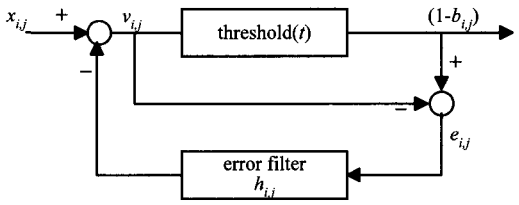

Fig. 2. Error diffusion system.

		7
1	5	3

Fig. 3. Error filter (Floyd-Steinberg's filter).

4. Blue noise masking

In this section, the algorithm[11~13] to generate a blue noise mask is presented. First, an initial blue-noise binary pattern $b[i,j,g]$ (two-dimensional binary pattern at gray level g) for some intermediate level $g(0<g<255$, assuming an 8-bit mask) is required. Using the filtering and swapping technique, such a pattern with blue-noise characteristics is obtained and used as the initial pattern. From this initial pattern, an initial mask $m[i,j]$ is generated, which when used to halftone the constant gray image of level g, produces the initial binary pattern $b[i,j,g]$.

Once level g is completed, level $g+1$ is processed (Fig. 4). For this level, the blue-noise pattern is created by converting the appropriate number (the total number of pixels in the binary pattern divide by the total number of levels) of 0s to 1s in the

previous pattern g. At the same time, the mask $m[i,j]$ is updated. This process is repeated until the mask has been updated for all the levels above g to level 255. Analogous procedures are used to construct the mask for all the levels below g to level 0. The resulting two-dimensional array $m[i,j]$ will be the final blue noise mask.

There is a significant constraint on the converting and swapping operation in this mask construction. In making a mask, the binary patterns at different levels are dependent. For example, in the upward construction process, all the 1s in the binary pattern for level g are contained in the binary pattern $g+1$, so when converting and swapping 1s and 0s, these common 1s shared by the two neighboring levels cannot be changed. The construction technique outlined above is quite general and has enabled the generation of masks with different properties such as 8-bit depth (level 0-255) and 12-bit depth (level 0-4095), small size (64 by 64) and large size (256 by 256), isotropic and anisotropic. There are two critical parts in designing a blue noise mask: the digital filters and the optimality issue.

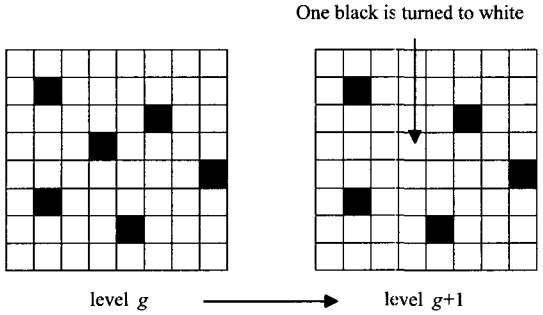

Fig. 4. Blue noise mask construction: from level g to $g+1$.

Ⅲ. PROPOSED MODEL-BASED DITHERING USING DOT PATTERN SELECTION

The above-mentioned dithering methods cannot fully represent the color component of an original image using the absorption properties of the inks. In this paper, a dot-pattern selection dithering method using a circular dot-overlap model and contrast sensitivity function (CSF) is proposed for representing the lightness of an original image as closely as possible. In the proposed method, a dot-pattern database is constructed based on a BNM using a circular dot-overlap model for the primary color inks. The size of each dot-pattern is $N_H \times N_W$, where N_H and N_W are decided according to the printer resolution that is used. In the dot-pattern database, the dot-pattern of a current pixel in the original image is selected to guarantee the blue-noise characteristic in each color using CSF. As a result, the proposed method is robust thereby preserving the original color and producing the best image quality.

1. Construction of dot-pattern database

The proposed algorithm modifies the weaknesses of the existing color dithering methods and constructs a dot-pattern database to represent the exact color component of the original image using a circular dot-overlap model.[14,15] A dot-pattern database is constructed independently for each CMY ink. The method for constructing the dot-pattern database is illustrated in Fig. 5.

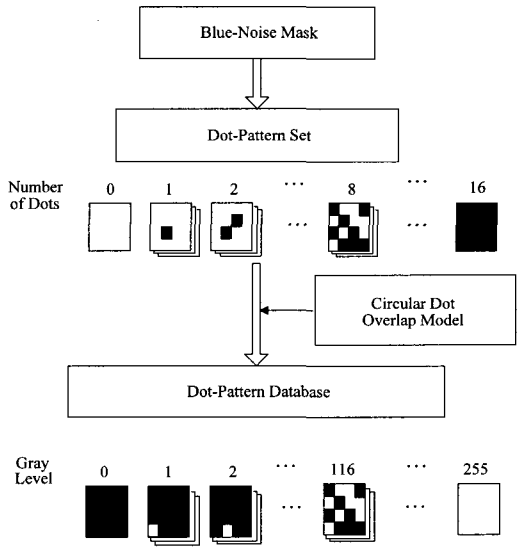

Fig. 5. Block diagram of construction of dot-pattern database.

The BNM used in the proposed method was developed by Parker[11~13] and its size is 256×256. By thresholding the BNM with each gray level, dot-profiles are constructed for every gray level. Using these dot-profiles, dot-patterns of $N_H \times N_W$ size for adjusting the resolution of the printer can then be recursively constructed by shifting 1 pixel. At this point, all previously constructed dot-patterns are excluded. The set of all the clipped dot-patterns is defined as the dot-pattern set.

As it is clipped from a BNM, the dot-pattern set already has blue-noise characteristics. When one pixel of the original image is dithered with the CMY dot-pattern databases independently, the color of the dot-pattern in the pixel of the reproduced image can be estimated as the average color of the dot-pattern in each CMY plane. The average color of one dot-pattern in a reproduced pixel, $P_{i,j} = \{P^C_{i,j}, P^M_{i,j}, P^Y_{i,j}\}$ is

$$P^C_{i,j} = \frac{1}{N_H N_W} \sum_x \sum_y p^C_{x,y}, \quad 0 \le x \le N_H,\ 0 \le y \le N_W,$$
$$P^M_{i,j} = \frac{1}{N_H N_W} \sum_x \sum_y p^M_{x,y}, \quad 0 \le x \le N_H,\ 0 \le y \le N_W,$$
$$P^Y_{i,j} = \frac{1}{N_H N_W} \sum_x \sum_y p^Y_{x,y}, \quad 0 \le x \le N_H,\ 0 \le y \le N_W, \tag{2}$$

where (i, j) is the location of a pixel in an original image and (x, y) is the location of a dot in the dot-pattern. The values of $p^C_{x,y}, p^M_{x,y}, p^Y_{x,y}$ are the gray levels of one dot in a $N_H \times N_W$ dot-pattern. In an ideal case, the gray level of each color dot is 255 and the value of a blank dot is 0. However, an actual printed image has smaller color values because the size of a dot is larger than that of an ideal case die to ink absorption. The proposed method modifies this error and represents the exact color values by applying a dot-overlap model to the dot-pattern. For color dithering, the dot-pattern set is sorted and divided into a subset according to color values between 0 and 255. This sorted dot pattern is defined as the dot-pattern database.

The dot-overlap model used in the construction of a dot-pattern database assumes that the dot is circular and its ideal size covers the total area of an ideal rectangular dot and its ink has no absorption. Then the radius of an ideal dot is $T/\sqrt{2}$. The dot overlap can be modeled as in Fig. 6.

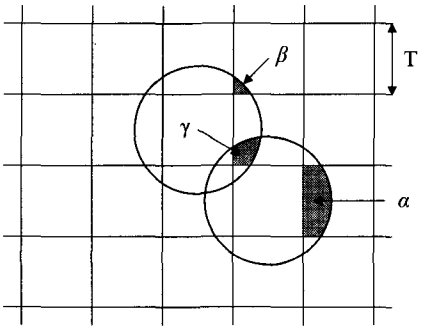

Fig. 6. Circular dot-overlap model of ink.

In an actual dithered image, the color value of each dot, $p^C_{x,y}, p^M_{x,y}, p^Y_{x,y}$ is

$$p^C_{x,y} = P(W_{x,y}) = \begin{cases} 255 \times (f_1\alpha - f_2\beta + f_3\gamma), & \text{if } b^C_{x,y} = 0 \\ 255, & \text{if } b^C_{x,y} = 255 \end{cases},$$
$$p^M_{x,y} = P(W_{x,y}) = \begin{cases} 255 \times (f_1\alpha - f_2\beta + f_3\gamma), & \text{if } b^M_{x,y} = 0 \\ 255, & \text{if } b^M_{x,y} = 255 \end{cases},$$
$$p^Y_{x,y} = P(W_{x,y}) = \begin{cases} 255 \times (f_1\alpha - f_2\beta + f_3\gamma), & \text{if } b^Y_{x,y} = 0 \\ 255, & \text{if } b^Y_{x,y} = 255 \end{cases}, \tag{3}$$

where $b^C_{x,y}, b^M_{x,y}, b^Y_{x,y}$ are color values of an ideal circular dot within a dot pattern and $W^C_{x,y}$ is a window which consists of $b^C_{x,y}$ and its neighbors as below.

$$W^C_{x,y} = \begin{vmatrix} b^C_{(x-1,y-1)} & b^C_{(x-1,y)} & b^C_{(x-1,y+1)} \\ b^C_{(x,y-1)} & b^C_{(x,y)} & b^C_{(x,y+1)} \\ b^C_{(x+1,y-1)} & b^C_{(x+1,y)} & b^C_{(x+1,y+1)} \end{vmatrix} \tag{4}$$

$W^M_{x,y}$ and $W^Y_{x,y}$ can be defined as in Eq. (4). The parameters α, β, and γ are the ratios of the color ink areas that are smeared into blank dots. f1 is the number of horizontally and vertically neighboring dots *i.e.* the number of 255 in the set $\{b_{(x-1,y)}, b_{(x,y-1)}, b_{(x,y+1)}, b_{(x+1,y)}\}$, f_2 is the number of diagonally neighboring dots (i.e. the number of 255 in the set $\{b_{(x-1,y-1)}, b_{(x-1,y+1)}, b_{(x+1,y-1)}, b_{(x+1,y+1)}\}$) that are not adjacent to the horizontally and vertically neighboring dots, and f_3 is the number of pairs of neighboring dots in which one is a horizontal neighbor and the other is a vertical neighbor.

The parameters α, β, and γ can be expressed in terms of the ratio ρ of the actual dot radius to the ideal dot radius $T/\sqrt{2}$ as follows:

$$\alpha = \frac{1}{4}\sqrt{2\rho^2-1} + \frac{\rho^2}{2}\sin^{-1}\left(\frac{1}{\sqrt{2}\rho}\right) - \frac{1}{2},$$
$$\beta = \frac{\pi\rho^2}{8} - \frac{\rho^2}{2}\sin^{-1}\left(\frac{1}{\sqrt{2}\rho}\right) - \frac{1}{4}\sqrt{2\rho^2-1} + \frac{1}{4},$$
$$\gamma = \frac{\rho^2}{2}\sin^{-1}\left(\sqrt{\frac{\rho^2-1}{\rho^2}}\right) - \frac{1}{2}\sqrt{2\rho^2-1} - \beta. \quad (5)$$

Because the characteristics of CMY inks are not the same, the ratio ρ is different for each CMY ink. Thus, by applying the ratio of each color, the average color value of a dot-pattern can be determined by Eq. (16) and the dot-pattern database of each CMY ink can be constructed by dividing the dot-patterns according to their color values from 0 to 255.

However, the size of a dot-pattern is $N_H \times N_W$. Therefore, a dot-pattern database has a limited ability to express all color values. Furthermore, a dot-pattern may not exist for some color values. These color values are, therefore, substituted with the dot-patterns of the closest color value that contains a few dot-patterns in both the up and down direction. The error due to this compensation can be reduced by a CSF dot-pattern selection algorithm that chooses an appropriate dot-pattern for the color value of a pixel in the original image.

Using the constructed dot-pattern database of CMY color inks, the original image can be dithered by randomly selecting the dot-pattern. The resulting dithered image represents the color values of the original image, however, it has a poor image quality as it has lost its blue-noise characteristic. Accordingly, a dot-pattern selection algorithm is needed to maintain the blue-noise characteristics.

2. Dot-pattern selection algorithm

In this paper, a dot-pattern selection algorithm is proposed that uses the characteristics of the CSF of the human visual system and considers the dot-patterns selected for neighboring pixels.

The CSF used in this paper is a model that approximates the response of the human visual system. This model is basically a low-pass filter and can be represented as follows:

$$V_{u,v} = \begin{cases} a(b + c\tilde{f}_{u,v})\exp(-(c\tilde{f}_{u,v})^d), & \text{if } \tilde{f}_{u,v} > f_{\max} \\ 1.0, & \text{otherwise} \end{cases} \quad (6)$$

where a = 2.2, b = 0.0192, c = 0.114, and d = 1.1; $\tilde{f}_{u,v}$ is the radial spatial frequency in cycles/degree and fmax is the frequency at which the function peaks. To make use of the human visual model, a conversion from cycles/degree to cycles/inch is required. Let P be the printer resolution, d the viewing distance from the eye to the object, N×N the size of the image, (u, v) a location in the FT (Fourier transform) domain and $\tilde{f}_u$, $\tilde{f}_v$ the spatial frequency in cycles/degree in the two dimensions. It can be shown that

$$\tilde{f}_u = \frac{2udP}{N}\tan(0.5°), \quad (7)$$

$$\tilde{f}_v = \frac{2vdP}{N}\tan(0.5°), \quad (8)$$

where a viewing distance of 20 inches is assumed.

The radial frequency can be given by

$$\tilde{f}_{u,v} = \sqrt{\tilde{f}_u^2 + \tilde{f}_v^2}\,. \tag{9}$$

To incorporate the decrease in sensitivity at angles other than horizontal and vertical, the radial frequency is scaled such as shown

$$\tilde{f}'_{u,v} \rightarrow \tilde{f}_{u,v} / s(\theta) \tag{10}$$

$$s(\theta) = (\frac{1-w}{2})\cos(4\theta) + (\frac{1+w}{2}) \tag{11}$$

where w is 0.7 as a symmetry parameter. $\tilde{f}'_{u,v}$ can then be substituted into Equation (20). With this conversion, the human visual model can be applied directly to a digital image. The CSF used in this paper is shown in Fig. 7.

Using this CSF, the difference between the visual responses to the original image and the dithered image can be computed as a numerical value. Therefore, an optimal dot-pattern for a color value can be selected from the database. The original image is processed in the order of C, M, and Y according to each selection method. This is because human vision is most sensitive cyan. As a result, for a dot-pattern selection from the cyan dot-pattern database, a selection algorithm using a CSF, FFT (fast Fourier transform), and RMSE (root mean squared error) is first carried out. Thereafter, magenta is processed using an algorithm that selects the maximal non-overlapped dot-pattern to the cyan dot pattern from the magenta database.

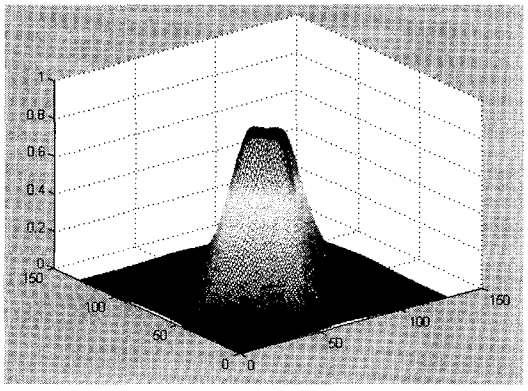

Fig. 7. CSF used in this paper.

At last, yellow is processed by an algorithm that selects the maximal non-overlapped dot-pattern to both the cyan and magenta dot-patterns from the yellow database. In order to reproduce the exact original colors, the dot-patterns selected during this process preserve the CMY color values estimated with a circular-dot overlap model.

In the proposed dot-pattern selection for cyan, in order to select the most appropriate dot-pattern for a current pixel from the cyan database, a local block method is used. A local 2×2 block of the original image and its corresponding halftone block of dot-patterns are compared using a CSF, FFT, and RMSE. The local block of the original cyan plane $B_{i,j}^{O\,C}$ can be represented as

$$B_{i,j}^{O\,C} = \begin{pmatrix} O_{i-1,j-1}^C & O_{i-1,j}^C \\ O_{i,j-1}^C & O_{i,j}^C \end{pmatrix}. \tag{12}$$

Where (i, j) means the location of the current pixel being processed and each component is the value of the cyan color in the pixel. The left and upper boundary pixels of the original cyan plane are randomly dithered using the cyan database. These pixels can be ignored, as they do not affect the quality of the dithered image. The corresponding halftone block of dot-patterns $B_{i,j}^{h\,C}$ can be represented as

$$B_{i,j}^{h\,C} = \begin{pmatrix} H_{i-1,j-1}^C & H_{i-1,j}^C \\ H_{i,j-1}^C & P_{i,j}^C \end{pmatrix} \tag{13}$$

where $H_{i-1,j-1}^C, H_{i-1,j}^C, H_{i,j-1}^C$ are the previously selected dot-patterns for the neighboring pixels. $P_{i,j}^C$ is the corresponding dot-pattern of the current pixel to be selected from the CMY dot-pattern database according to the

original cyan value. The size of $B^{h\,C}_{i,j}$ is 2NH× 2NW. So, $B^{O\,C}_{i,j}$ is interpolated to have the same size as $B^{h\,C}_{i,j}$, where $B^{O\,C}_{i,j}$ is interpolated as $I^{O\,C}_{i,j}$ by using the zero-order interpolation method. Fig. 8 shows the dot-pattern selection process of cyan with a 300 dpi printer. 300 dpi means that the size of the dot-pattern is 4×4, i.e. $N_H = N_W = 4$. Therefore, $B^{O\,C}_{i,j}$ can be interpolated as a ratio of 4:1. The interpolated block $I^{O\,C}_{i,j}$ and halftone block $B^{h\,C}_{i,j}$ are fast Fourier transformed, and the CSF is applied to both FFT results. The RMSE can then be computed as follows.

$$RMSE = \frac{1}{4N_H N_W}\sum_u\sum_v \sqrt{(F^{O\,C}_{u,v}\times V_{u,v} - F^{h\,C}_{u,v}\times V_{u,v})^2}\,,$$

$$F^{O\,C}_{u,v} = FFT\left\{I^{O\,C}_{i,j}\right\},\quad F^{h\,C}_{u,v} = FFT\left\{B^{h\,C}_{i,j}\right\},\qquad (14)$$

$$1\le u\le 2N_H,\qquad 1\le v\le 2N_W\,,$$

where $V_{u,v}$ is the CSF and FFT{ } is fast Fourier transformation processor. A dot pattern $P^C_{i,j}$ of the minimal RMSE is selected as a the dot-pattern $H^C_{i,j}$ of the current pixel which is faithful to the original cyan value and used in the dot-pattern selection of the next pixel. Fig. 9 shows the global structure of the selection algorithm for a cyan dot-pattern.

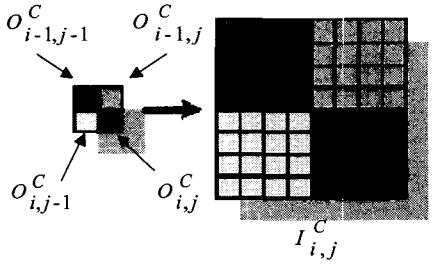

(a)

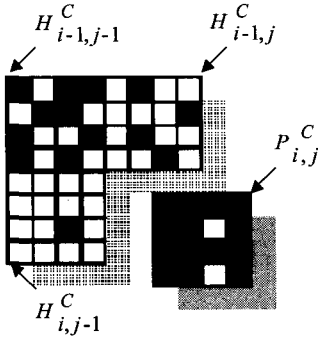

(b)

Fig. 8. Dot-pattern selection process of cyan plane with 300 dpi printer: (a) block of original cyan and 1:4 interpolated block, (b) dot-pattern block.

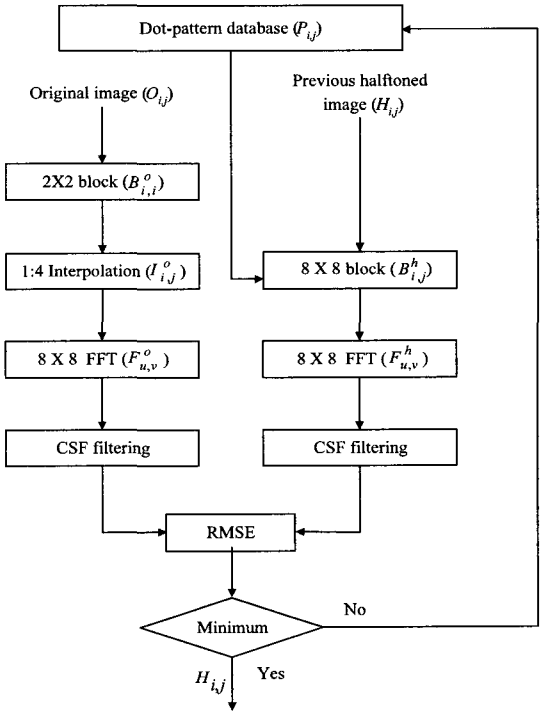

Fig. 9. Global structure of dot-pattern selection algorithm.

After a cyan dot-pattern is selected using the above method, in order to minimize any overlapping among the dot-patterns, a slightly different dithering block is used for the magenta and yellow planes, as follows.

$$B_{i,j}^{h\ M}=\begin{pmatrix}(H_{i-1,j-1}^{M}\ OR\ H_{i-1,j-1}^{C}) & (H_{i-1,j}^{M}\ OR\ H_{i-1,j}^{C})\\ (H_{i,j-1}^{M}\ OR\ H_{i,j-1}^{C}) & (P_{i,j}^{M}\ OR\ H_{i,j}^{C})\end{pmatrix}, \quad (15)$$

$$B_{i,j}^{h\ Y}=\begin{pmatrix}(H_{i-1,j-1}^{Y}\ OR\ H_{i-1,j-1}^{M}\ OR\ H_{i-1,j-1}^{C}) & (H_{i-1,j}^{Y}\ OR\ H_{i-1,j}^{M}\ OR\ H_{i-1,j}^{C})\\ (H_{i,j-1}^{Y}\ OR\ H_{i,j-1}^{M}\ OR\ H_{i,j-1}^{C}) & (P_{i,j}^{Y}\ OR\ H_{i,j}^{M}\ OR\ H_{i,j}^{C})\end{pmatrix}, \quad (16)$$

where OR means the Boolean OR operation and C means cyan, M magenta, and Y yellow. Using the decided dithering block for magenta and yellow, the previously explained algorithm is then used for the dot-pattern selection for the magenta and yellow planes.

The speed of the proposed method using a CMY dot-pattern database depends on the number of dot-patterns for each color value in the database. Therefore, in order to decrease the processing time, the number of dot-patterns should be decreased. In the proposed method, the number of dot-patterns is decreased by a statistical method that selects a certain number of dot-patterns in order of their frequency of use. Therefore, for 9 different experimental images, the statistical value of a dot-pattern is computed, then using this value, the top 5, 2, or 1 dot-patterns for each color value are determined.

The proposed method can faithfully represent the color of an original image and produces an improved image quality with a similar speed to that of the ordered dither method.

Ⅳ. EXPERIMENTAL RESULTS

For the test of the proposed method, Macbeth color-chart was used as reference colors. To measure colors displayed on the monitor and printed on the printer, Minolta CA-100 and Minolta CM-3600d were also used respectively. For choosing the optimum number of the dot patterns, several halftone images using different number of dot patterns were objectively evaluated by color difference (ΔE_{ab}^{*}). The tested numbers of dot patterns were 5, 2, and 1. The number 1 was so small that the binary pattern could not be well distributed, and therefore, some block artifacts were appeared. The required memory size for halftoning database was justly increased according to increasing the dot pattern number. Therefore, the five dot patterns were used for halftoning.

Fig. 10 and Fig. 11 show images printed by various halftoning techniques. Here, (a) is the result of ordered dither, (b) is the result of error diffusion, (c) is the result of blue noise masking, (d) is the result of proposed dot-pattern selection method. In Fig. 10 and Fig. 11 (a), (b), and (c), the colors were degraded due to the overlapping of printing dots. And (a) shows blocking effect in the smooth region. As the result of applying the proposed method, Fig. 10 and Fig. 11 (d) had visual characteristic of blue noise mask and reproduced accurate gray levels. Thus, the proposed method can substantially reproduce the color values of the pixels in original image and obtain better image quality.

To compare the halftoning techniques, color difference (ΔE_{ab}^{*}) was calculated. The reproduced colors were measured by spectrophotometer. From the result, ΔE_{ab}^{*} was calculated as follows;

$$\Delta E^{*}_{ab}=\sqrt{(L^{*}o-L^{*}R)^{2}+(a^{*}o-a^{*}R)^{2}+(b^{*}o-b^{*}R)^{2}} \quad (30)$$

where $L_{O}^{*}a_{O}^{*}b_{O}^{*}$ is CIEL*a*b* values measured on the monitor, $L_{R}^{*}a^{*}b^{*}$ is CIEL*a*b* values measured on the printer. Table 1 shows the comparison of the ΔE_{ab}^{*} in the Macbeth color chart by using two conventional methods and the proposed method. The two conventional methods are error diffusion and

Table 1. The comparison of ΔE_{ab}^{*} between colors displayed on the monitor and colors reproduced on the printer.

	Ordered dither	Error diffusion	Blue noise masking	The proposed method
ΔE_{ab}^{*}	22.13	21.88	19.96	14.20

blue noise masking. In the table, the proposed algorithm takes less error than the conventional methods.

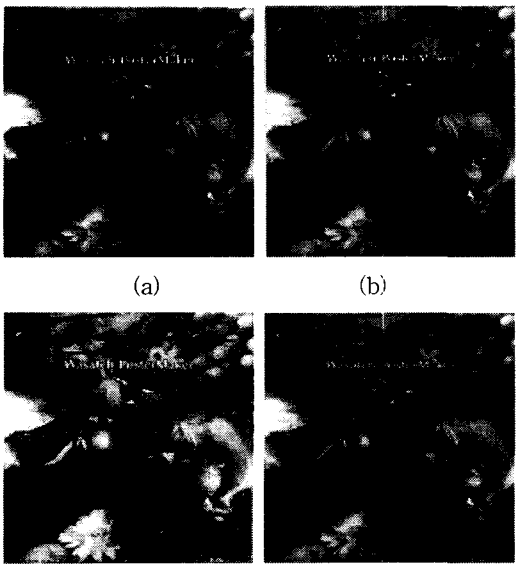

(a) (b)

(c) (d)

Fig. 10. Fresh image printed by various halftoning techniques. (a) Ordered dither. (b) Error diffusion. (c) BNM. (d) The proposed method.

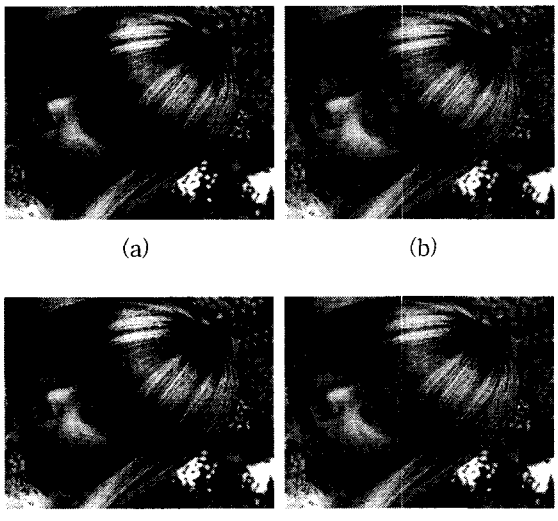

(a) (b)

(c) (d)

Fig. 11. Apple image printed by various halftoning techniques. (a) Ordered dither. (b) Error diffusion. (c) BNM. (d) The proposed method.

V. CONCLUSION

In order to improve the visual quality of color halftoning, model-based dithering of dot-pattern selection was proposed. The proposed method could represent linear color change, because it considered the problem of dot-overlap. To solve the problem of dot-overlap, the gray levels of dot-pattern sets were calculated using a circular dot-overlap model and then measured by a spectrometer. Thereafter, the dot-pattern sets were reordered according to the results. In this process, in order to improve the visual quality of the color dithering, the contrast sensitivity function (CSF) of the human visual system was used. As a result, the proposed techniques enable limited-color output devices to display and print high quality color images.

REFERENCES

[1] R. Ulichney, Digital Halftoning, *The MIT Press Cambridge*, 1987.

[2] H. R. Kang, *Color Technology For Electronic Image Devices*, SPIE Optical Engineering Press, pp. 122~126, 1996.

[3] D. E. Knuth, "Digital Halftones by Dot Diffusion," *ACM Trans. on Graphics*, vol. 6, no. 4, pp. 245~273, October 1987.

[4] R. S. Gentile, E. Walowit, and J. P. Allebach, "Quantization and Multilevel Halftoning of Color Images for Near-Original Image Quality," *Journal of Optical Society in America A*, no. 7, pp. 1019~1026, 1990.

[5] H. G. Lamming and W. L. Rhodes, "A Simple Method for Improved Color Printing of Monitor Images," *ACM Trans. on Graphics*, vol. 9, no. 4, pp. 345~375, October 1990.

[6] S. C. Wells, G. J. Williamson, and S. E. Carrie, "Dithering for 12-Bit True-Color Graphics," *IEEE Computer Graphics & Application*, pp.

18~29, September 1991.

[7] K. M. Kim, C. S. Lee, E. J. Lee, and Y. H. Ha, "Color Image Quantization and Dithering Method Based on Human Visual System Characteristics," *The Journal of Imaging Science and Technology*, vol. 40, no. 6, pp. 502~509, 1996.

[8] R. Eschbach and K. T. Knox, "Error-Diffusion Algorithm with Edge Enhancement," *Journal of Optical Society in America A*, vol. 8, no. 12, pp. 1844~1850, December 1991.

[9] R. Ulichney, "The Void-and-Cluster Method for Dither Array Generation," *Human Vision, Visual Processing, and Digital Display IV*, vol. 1913, pp. 332~343, 1993.

[10] I. Amidror, R. D. Hersch, and V. Ostromoukhov, "Spectral Analysis and Minimization of Moire Patterns in Color Separation," *Journal of Electronic Imaging*, vol. 3, no. 3, pp. 295~317, July 1994.

[11] Q. Yu, M. Yao, and K. J. Parker, "Color Halftoning with Blue Noise Masks," *Fourth Color Imaging Conference: Color Science, Systems and Applications*, pp. 77~79, 1996.

[12] Q. Yu and K. J. Parker, "Adaptive Color Halftoning for Minimum Perceived Error Using the Blue Noise Mask," *Color Imaging Conference: Device-Independent Color, Color Hard Copy, and Graphic Arts II*, vol. 3018, pp. 272~276, 1997.

[13] T. Mitsa and K. J. Parker, "Digital Halftoning Technique Using a Blue-Noise Mask," *Journal of Optical Society in America A*, vol. 9, no. 11, pp. 1920~1929, November 1992.

[14] T.N. Pappas and D. L. Neuhoff, "Least-Squares Model-Based Halftoning," *Human Vision, Visual Processing, and Digital Display III*, vol. 1666, pp. 165~176, 1992.

[15] T. N. Pappas, D. L. Neuhoff, "Printer Model and Error Diffusion," *IEEE Trans. On Image Processing*, vol. 4, no. 1, pp. 66~80, 1995.

저 자 소 개

李 採 守(正會員)

1968年 10月 15日生. 1994年 경북대학교 전자공학과(공학사), 1996年 경북대학교 대학원 전자공학과(공학석사), 2000年 경북대학교 대학원 전자공학과(공학박사). 1999年 ~ 현재 경운대학교 소프트웨어공학전공 전임강사. 주관심분야는 디지털 칼라처리, 칼라 프린팅, 장치간 칼라 일치 등임

朴 洋 佑(正會員)

1966年 4月 26日生. 1988年 경북대학교 전자공학과(공학사), 1990年 경북대학교 대학원 전자공학과(공학석사), 2000年 경북대학교 대학원 전자공학과(공학박사). 1997年 ~ 현재 경운대학교 소프트웨어공학전공 조교수. 주관심분야는 칼라 영상처리, 칼라 프린팅, 칼라 양자화 등임

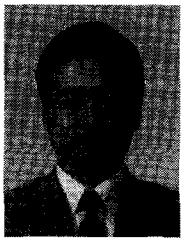

張 周 錫(正會員)

1954年 7月 13日生. 1982年 영남대학교 전자공학과(공학사), 1984年 영남대학교 대학원 전자계산학과(공학석사), 1997年 영남대학교 대학원 전자계산학과(공학박사). 1997年 ~ 현재 경운대학교 소프트웨어공학전공 교수. 주관심분야는 영상처리, 모폴로지 등임

嚴 泰 億(正會員) 第 36券 S編 第 5號 參照
현재 구미기능대학교 전자과 부교수

河 永 浩(正會員) 第 32券 B編 第 12號 參照
현재 경북대학교 전자전기공학부 교수